Preprints of the 21st IFAC World Congress (Virtual)
Berlin, Germany, July 12-17, 2020

Are External Magnetic Disturbances Suppressed by Magnetometer Noise when Estimating a Nanosatellite's Rotational Motion?

Demet Cilden-Guler[*], Zerefsan Kaymaz[**], Chingiz Hajiyev[***]

Faculty of Aeronautics and Astronautics, Istanbul Technical University, Istanbul, Turkey
(e-mails: [*]cilden@itu.edu.tr, [**]zerefsan@itu.edu.tr, [***]cingiz@itu.edu.tr).

Abstract: In this study, a three-axis magnetometer based attitude estimation algorithm that includes external magnetic field model is presented. The magnetic fields from the external sources are considered in the geomagnetic field model used in the attitude estimation algorithm and not treated as error sources on the magnetometer. By this way, it was aimed to model the magnetometer better by taking into account the effects of the space environment and perform a higher accuracy in the estimation of the rotational motion of the satellite. However, a problem arose such that the magnetometer sensor noise levels used in the attitude estimations appear to mask the effects of the external magnetic field. The fact that with the developing technologies in micro-electro-mechanical systems, the magnetometer noise might be keep decreasing, led us to investigate the magnitude of the noise level that would suppress the external field.

Keywords: satellite attitude estimation, magnetospheric substorms, external magnetic field, magnetometer noise.

1. INTRODUCTION

Since the magnetometers are inexpensive, reliable and lightweight, they are the most widely used sensors for determining the attitude angles of nanosatellites in low Earth orbit. The difference between the predicted and observed magnetic field vectors affects the accuracy of the estimation of the nanosatellite's attitude. The International Geomagnetic Reference Field (IGRF) model (Thébault et al., 2015) is used for the attitude estimation systems in most cases, but when the geomagnetic activity occurs, the difference between the sensor and the model increases (Cilden-Guler et al., 2018). Therefore, models containing external magnetic field variations caused by solar wind and/or magnetic storms and magnetospheric substorms are of great importance in accurately determining the satellite's attitude. A general application of modeling external magnetic field is to treat the magnetic anomalies as error sources like noise or bias on the magnetometer measurements and exclude these errors by estimating them in the augmented states (Takaya Inamori et al., 2016; Takaya Inamori and Nakasuka, 2012). On the other hand, the external field can be used both in the measurement and the magnetic field model as an additional term. In (Cilden-Guler et al., 2018), IGRF and T89 (Tsyganenko, 1989) geomagnetic field models were compared in order to study the errors resulting from the magnetic field representation. In this study, T89 model gave closer predictions to the observations, especially during magnetically active times compared to the IGRF-12 model. However, various magnetometer noise levels were not considered in that study. Therefore, the magnetic field deviations created by the geomagnetic disturbances might be suppressed by the critical noise level in which case the external field effects on attitude estimation would be underestimated since they will be dependent to the noise level.

To simulate the magnetometer, a realistic space environment conditions obtained by magnetospheric models are considered. In the absence of such models, deviations from the geomagnetic field due to external conditions are often treated as bias or noise in the simulated magnetometer (Archer et al., 2015; T Inamori et al., 2010; Takaya Inamori et al., 2016; Takaya Inamori and Nakasuka, 2012) in addition to the measurement noise contained in the magnetometers sensors. However, the measurement noises can mask the effects of external sources on the geomagnetic field depending on the noise level. With developing technologies in micro-electro-mechanical systems, noise levels in magnetometers have decreased, leading to an increase of the external magnetic field effects on the attitude of satellites. For example, in (Matandirotya et al., 2013) , three commercially available fluxgate magnetometers were evaluated with power efficiency, weight, noise, linearity and adaptability criteria. One of the Fluxgate magnetometers has passed environmental tests and is recommended for the CubeSat installation. The performance characteristics of the magnetometer were 0.7 nT (RMS) noise at 12.83 Hz, ± 2 nT and 0.03 W power consumption above ± 60000 nT nonlinearity. This magnetometer noise level is much smaller than the default magnetometer measurement noise and the standard deviation is around 100 nT (Zhang et al., 2015). In this study, we take into account the fact that the noise levels in the magnetometers decrease with the new technologies developed in the micro-electro-mechanical systems, will expose the external magnetic field more to the attitude of the satellites.

This is a follow-up study of (Cilden-Guler et al., 2019) in which a series of magnetometer sensor noise levels are implemented for magnetically active event to evaluate the external magnetic field and magnetometer measurement noises. In this study, the purpose is to validate the critical

magnetometer measurement noise level assumed in the spacecraft attitude estimation. It is important to emphasize that the magnetic field models commonly used for attitude estimation e.g. IGRF do not take into account the external sources which might be misleading in the attitude estimation algorithm as it would treat the external magnetic field as an additional noise on the sensor. Yet, in reality, the variations in the magnetic field are caused by a physical phenomenon such as a magnetospheric substorm event. Therefore, the algorithm is generated using the T89 model (Tsyganenko, 1989, 2008) that includes the external effects. The structure of the paper is as follows. First, the rotational motion of the satellite is given. This is followed by the magnetometer measurements and the filtering technique for the attitude estimation algorithm. After this, the analysis and the results are demonstrated. Finally, in the last section, a summary, and conclusions of the paper are presented.

2. SATELLITE'S ROTATIONAL MOTION

The state vector for the continuous-time dynamic model is composed of attitude angles of the nanosatellite as,

$$\mathbf{x} = \begin{bmatrix} \phi & \theta & \psi \end{bmatrix}^T, \tag{1}$$

where ϕ is roll, θ is pitch, ψ is yaw. Attitude angles are propagated in time as,

$$\begin{bmatrix} \dot{\phi} \\ \dot{\theta} \\ \dot{\psi} \end{bmatrix} = \begin{bmatrix} 1 & s(\phi)t(\theta) & c(\phi)t(\theta) \\ 0 & c(\phi) & -s(\phi) \\ 0 & s(\phi)/c(\theta) & c(\phi)/c(\theta) \end{bmatrix} \begin{bmatrix} p \\ q \\ r \end{bmatrix}, \tag{2}$$

where $c(\cdot)$, $s(\cdot)$, and $t(\cdot)$ are cosine, sine and tangent functions, and $\boldsymbol{\omega}_{BR} = \begin{bmatrix} p & q & r \end{bmatrix}^T$ is the angular velocity vector in body frame with respect to the reference frame. The angular velocities $(\boldsymbol{\omega}_{BI})$ in the body frame can be expressed with respect to the inertial coordinates as,

$$\boldsymbol{\omega}_{BI} = \begin{bmatrix} \omega_x & \omega_y & \omega_z \end{bmatrix}^T, \tag{3}$$

with a relationship of,

$$\boldsymbol{\omega}_{BR} = \boldsymbol{\omega}_{BI} + \mathbf{A}\begin{bmatrix} 0 & -\omega_o & 0 \end{bmatrix}^T, \tag{4}$$

where ω_o orbital angular velocity which can be computed as,

$$\omega_o = \left(\mu / r_0^3\right)^{1/2}, \tag{5}$$

using μ-gravitational constant, r_0- distance between the satellite and Earth's centers. $\mathbf{A}$ represents the transformation matrix from orbit to body frame.

Dynamic equations from the principle of conservation of angular momentum are,

$$J_x \frac{d\omega_x}{dt} = N_x + \left(J_y - J_z\right)\omega_y\omega_z, \tag{6a}$$

$$J_y \frac{d\omega_y}{dt} = N_y + \left(J_z - J_x\right)\omega_z\omega_x, \tag{6b}$$

$$J_z \frac{d\omega_z}{dt} = N_z + \left(J_x - J_y\right)\omega_x\omega_y, \tag{6c}$$

where J_x, J_y and J_z inertial moment elements, N_x, N_y and N_z are the disturbances affecting the satellite.

3. MAGNETOMETER MEASUREMENTS

In this study, magnetometer measurements are used in order to estimate the satellite's attitude angles. In the estimation algorithm, a magnetic field model should also be used in addition to the magnetometer measurements.

IGRF (International Geomagnetic Reference Field) can be used as the geomagnetic field model; its inputs are date and position of the satellite (Thébault et al., 2015; Wertz, 1988, pp. 779–782):

$$\mathbf{B}_{\text{IGRF}}(\bar{r}, \text{colat}, \text{lon}, t) = -\nabla\{a\sum_{n=1}^{N}\sum_{m=0}^{n}\left(\frac{a}{\bar{r}}\right)^{n+1} \times \ \ldots$$
$$\left[g_n^m(t)c\left(m\ \text{lon}(t)\right) + h_n^m(t)s\left(m\ \text{lon}(t)\right)P_n^m\left(c\left(\text{colat}(t)\right)\right)\right]\}, \tag{7}$$

where $\mathbf{B}_{\text{IGRF}}$ is the predicted magnetic field in nanoTesla (nT), $\bar{r}$ is the distance between the mass centres of the satellite and Earth, colat(t) is the co-latitude, lon(t) is the longitude, $P_n^m\left(\text{c}\left(\text{colat}(t)\right)\right)$ are the Schmidt quasi-normalized associated Legendre polynomials of degree n and order m, $a = 6371.2$ km is the geomagnetic conventional Earth's mean reference spherical radius, g_n^m and h_n^m are the Gaussian coefficients given in units of nT (Thébault et al., 2015).

As the magnetometer measurements are affected by the external magnetic field sources, it is the best way to represent such measurements using a model that includes them. That's why, for the magnetic field model, T89 model (Tsyganenko, 1989) was selected. T89 is composed of two parts as:

$$\mathbf{B}_{\text{T89}_k} = \mathbf{B}_{\text{IGRF}_k} + \mathbf{B}_{\text{ext}_k}, \tag{8a}$$

$$\mathbf{B}_{\text{ext}} = \mathbf{B}_{ring} + \mathbf{B}_{tail} + \mathbf{B}_{mp} + \mathbf{B}_{FC}, \tag{8b}$$

where $\mathbf{B}_{\text{T89}}$ represents magnetic field vector from T89 model including the IGRF model outputs $(\mathbf{B}_{\text{IGRF}})$ and external magnetic field contribution $(\mathbf{B}_{\text{ext}})$. IGRF model considers the internal part of the geomagnetic field of the Earth and updates its constants every five years (Thébault et al., 2015). On the other hand, T89 model utilizes large data sets from a variety of satellites.

$\mathbf{B}_{\text{ext}}$ includes effects from magnetospheric ring current $(\mathbf{B}_{ring})$, tail current $(\mathbf{B}_{tail})$, magnetopause currents $(\mathbf{B}_{mp})$, and field aligned currents $(\mathbf{B}_{FC})$ (Tsyganenko, 1989, 1995, 2002).

Since the external magnetic field $(\mathbf{B}_{\text{ext}})$ is overlaid on the main geomagnetic field, T89 gives the total geomagnetic field at the specified location. By this way the model brings in the effects from magnetospheric ring current, tail current, magnetopause currents, and Region 1 and 2 field. In order to determine the magnetospheric activity level, K_p index is used. The index can have the values in Table 1 and used as I_{opt} in T89.

Table 1. K_p Index Interval

I_{opt}	1	2	3	4	5	6	7
K_p	0	1	2	3	4	5	6+

The magnetometer measurements are simulated using the transformed geomagnetic field model vector and the measurement noise vector and generalized as,

$$\mathbf{B}_{m_k} = \mathbf{A}_k \mathbf{B}_{o_k} + \mathbf{v}_{B_k}, \tag{9}$$

where $\mathbf{B}_o$ is the Earth's magnetic field vector components in the orbital frame that were found using a geomagnetic field model which equals to $\mathbf{B}_{\text{ext}}$ in this study, $\mathbf{B}_m$ is the magnetometer measurements in the spacecraft's body frame, $\mathbf{v}_B$ is the magnetometer measurement noise with zero-mean.

4. EXTENDED KALMAN FILTER BASED ATTITUDE ESTIMATION ALGORITHM

The attitude angles of the nanosatellite are estimated by using Kalman filtering based algorithm using magnetometer measurements and magnetic field model (see Fig. 1). The scheme shows the measurement related part of the algorithm. The important part is to include the geomagnetic activity index in order to include the external magnetic field anomalies.

For the filter, the attitude estimation problem is formulated using the standard discrete-time nonlinear state-space model

$$\mathbf{x}_k = f(\mathbf{x}_{k-1}) + \mathbf{w}_k, \tag{10a}$$

$$\mathbf{y}_k = h_k(\mathbf{x}_k) + \mathbf{v}_k, \tag{10b}$$

where $f(\cdot)$ and $h(\cdot)$ are nonlinear dynamic and measurement functions respectively, $\mathbf{x}$ is the state vector, $\mathbf{w}$ is a zero-mean Gaussian noise with covariance $\mathbf{Q}$, $\mathbf{y}$ is measurement vector, and $\mathbf{v}$ is a zero-mean Gaussian noise with covariance $\mathbf{R}$.

In the estimation algorithm based on the described system and measurements in (10), the approximations of the prediction and update stages can be found based on the EKF (Psiaki et al., 1990). The estimation value can be found as,

$$\hat{\mathbf{x}}_k = \hat{\mathbf{x}}_{k|k-1} + \mathbf{K} \times \left\{ \mathbf{y}_k - h\left(\hat{\mathbf{x}}_{k|k-1}\right) \right\} \tag{11}$$

The extrapolation value of the dynamic function can be found as,

$$\hat{\mathbf{x}}_{k|k-1} = f(\mathbf{x}_k) \tag{12}$$

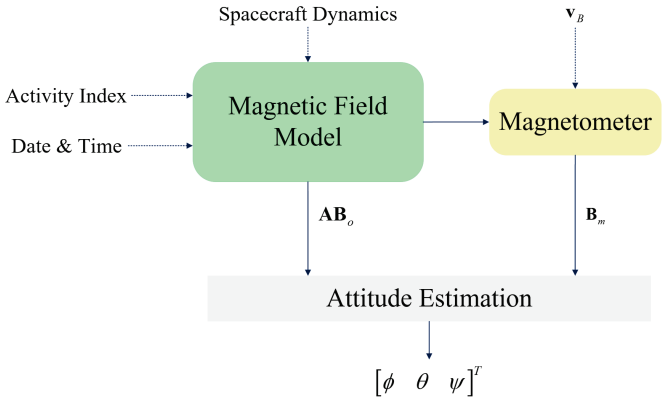

Fig. 1. Attitude estimation algorithm flow chart using only magnetometer.

Filter-gain of the EKF is,

$$\mathbf{K}_k = \mathbf{P}_{k+1|k}\mathbf{H}_k \times \left[\mathbf{H}_k \mathbf{P}_{k+1|k} \mathbf{H}_k^T + \mathbf{R} \right]^{-1} \tag{13}$$

where $\mathbf{H}_k = \dfrac{\partial h\left(\hat{\mathbf{x}}_{k|k-1}\right)}{\partial \hat{\mathbf{x}}_{k|k-1}}$ is the partial derivatives of the measurement function with respect to the states.

The covariance matrix of the extrapolation error is,

$$\mathbf{P}_{k+1|k} = \frac{\partial f\left(\hat{\mathbf{x}}_k\right)}{\partial \hat{\mathbf{x}}_k} \mathbf{P}_{k|k} \times \frac{\partial f^T\left(\hat{\mathbf{x}}_k\right)}{\partial \hat{\mathbf{x}}_k} + \mathbf{Q} \tag{14}$$

The covariance matrix of the filtering error is,

$$\mathbf{P}_{k+1|k+1} = \left[\mathbf{I} - \mathbf{K}_k \mathbf{H}_k \right] \mathbf{P}_{k+1|k} \tag{15}$$

The extended Kalman filter described in (11) – (15) is based on the traditional approach. In this study, only magnetometer measurements are used as defined in (8),

$$\mathbf{y}_k = \mathbf{B}_{m_k}. \tag{16}$$

The magnetic field model is used in composing the measurement matrix $\mathbf{H}_k$.

5. ANALYSIS AND RESULTS

A nanosatellite orbiting around Earth with the principal moments of inertia $\mathbf{J} = \text{diag}\left(2.1\times10^{-3} \quad 2.0\times10^{-3} \quad 1.9\times10^{-3}\right)$ kg m^2 is considered in this study. The satellite has only one attitude sensor which is a three-axis magnetometer. For the magnetometer measurements, the sensor noise is characterized by zero-mean Gaussian white noise with variable standard deviation in nT. The system and measurement noise covariance matric is taken as $\mathbf{Q} = \text{diag}\left(\left[0.001 \quad 0.001 \quad 0.001\right]\right)$. An average external torque is applied on the spacecraft rotational motion dynamics with a constant value of 3.6×10^{-7} Nm .

First, we give the critical noise standard deviation level of the magnetometer measurements in Fig. 2 by comparing it with mean magnetic field values of the external sources over time (constant line). The external magnetic field contribution $\left(\bar{B}_{ext}\right)$ is calculated at $\sigma = 0$ by taking average over time. Measurement noise $\left(\bar{v}_B\right)$ is averaged over time for every σ value (from 0 to 100). The external magnetic field is modeled for a magnetically active time period using T89 model. The exceeding point of the noises with respect to the external field is around 35 nT noise standard deviation. It means that the external magnetic field will be masked completely around 70 nT. However, their effects on attitude estimation will be revealed as other parameters get involved in the estimation procedure discussed in Section 4. For this reason, we expect that overlapping of all magnetic anomalies affecting the satellite might happen at a lesser noise level than 70 nT.

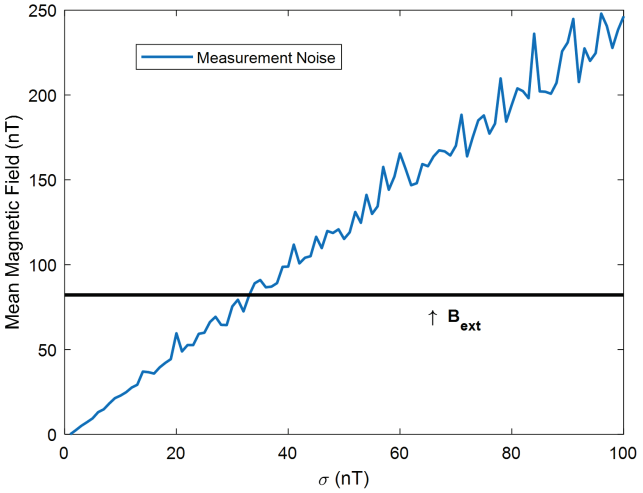

Fig. 2. Mean magnetic field values of the measurement noise and external magnetic field.

In order to further investigate the critical noise level, normalized root mean square errors (NRMS) (see Fig. 4) and the total unitized errors (see Fig. 5) are used.

NRMS of the attitude estimations is given in Fig. 4 with increasing standard deviation on the magnetometer measurements. The scattered error data are fitted into a linear line using the least square approximation, which shows the trend of the errors increases with the standard deviation as expected.

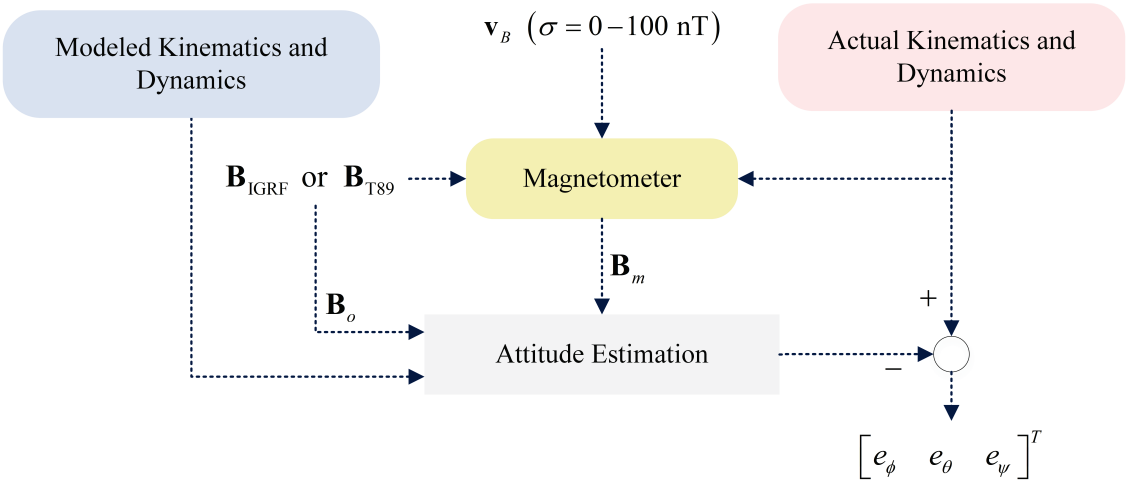

Fig. 3. Block diagram on calculating attitude estimation errors based on only magnetometer.

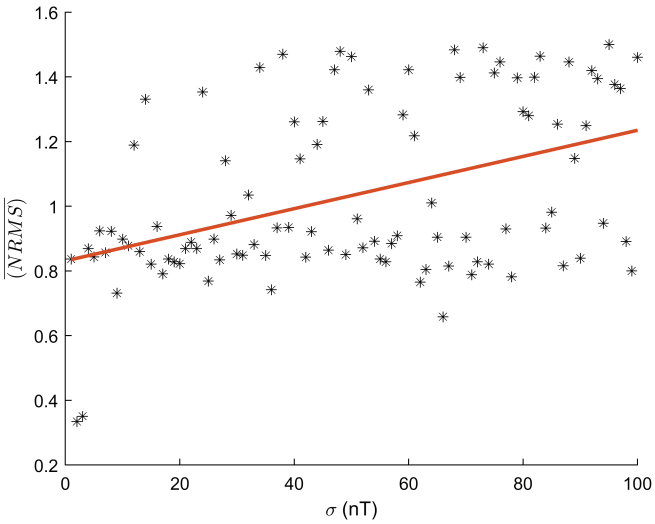

Fig. 4. Mean NRMS error of attitude estimations with respect to the measurement noise standard deviation.

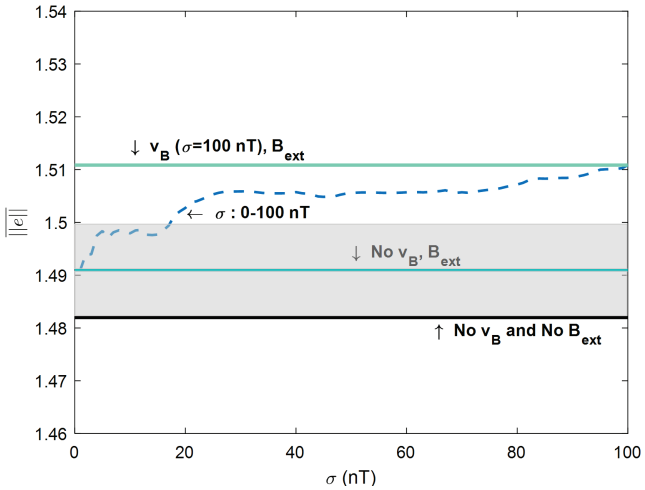

Fig. 5. Error norm changes with respect to the measurement noise standard deviation for the cases -with or without- the measurement noise and external magnetic field.

The normalized error means of the attitude estimations calculated using absolute errors (Fig. 3) shown in Fig. 5 are calculated as,

$$\overline{\|e\|} = \frac{\sum_k \frac{|e_{\phi_k}| + |e_{\theta_k}| + |e_{\psi_k}|}{\sqrt{\left(e_{\phi_k}^2 + e_{\theta_k}^2 + e_{\psi_k}^2\right)}}}{n} \tag{17}$$

where k is the time stamp, and n is the number of samples.

In Fig. 5, we plotted three constant lines each of which corresponds to different combination of measurement noise standard deviation and external field pair cases. These are:

- The case with no noise on the measurements or no external field in the environment,
  - Calculated at $\sigma = 0$.
- The case with no noise on the measurements but there is an external field in the environment,
  - Calculated at $\sigma = 0$.
- The case with a noise on the measurements with 100 nT standard deviation and an external field in the environment,
  - Calculated at $\sigma = 100$.

$\mathbf{v}_B$ is the measurement noise defined in (9). All the cases are applied on the same system, same magnetic field model for the filter, and same filter configuration. The dashed line in Fig. 5 shows the changes in the error output with respect to the standard deviation. The starting and the ending points of the dashed line, which includes the external magnetic field in the algorithm, are pointed out by using the straight lines as 0 nT and 100 nT standard deviation on the magnetometer measurements. The gray area demonstrates the masking region exceeds the external effects around 20 nT standard deviation.

6. CONCLUSIONS

The attitude angles of a nanosatellite are estimated using an extended Kalman filter. The filter uses the satellite's dynamical equations of motion and one three-axis magnetometer as the attitude sensor. For the magnetic field, a model that includes external anomalies is considered in order not only to better model the magnetic field for the simulation and the magnetometer sensor but also for the estimation accuracy. However, as the nanosatellites generally use low-accurate magnetometer sensors, their noise levels might suppress the whole effect of the external part of the magnetic fields. That is why the magnetometer measurement's noise level that is affecting the nanosatellite's attitude estimation more than the external magnetic field is determined in this study. The results show that the magnetic anomalies can be revealed if the measurement noise standard deviation is under 70 nT because of the difference in the magnetic field levels. However, the standard deviation of the measurement noise masking the external field less than 20 nT.

ACKNOWLEDGMENTS

The author D. Cilden-Guler is supported by ASELSAN (Military Electronic Industries) and TUBITAK (Scientific and Technological Research Council of Turkey) PhD Scholarships. We thank Nikolai Tsyganenko for sharing his model with the public.

REFERENCES

Archer, M. O., Horbury, T. S., Brown, P., Eastwood, J. P., Oddy, T. M., Whiteside, B. J., and Sample, J. G. (2015). The MAGIC of CINEMA: first in-flight science results from a miniaturised anisotropic magnetoresistive magnetometer. *Ann. Geophys*, *33* , 725–735. https://doi.org/10.5194/angeo-33-725-2015

Cilden-Guler, D., Kaymaz, Z., and Hajiyev, C. (2018). Evaluation of Geomagnetic Field Models using

Magnetometer Measurements for Satellite Attitude Determination System at Low Earth Orbits: Case Studies. *Advances in Space Research*, *61* (1), 513–529. https://doi.org/10.1016/j.asr.2017.10.041

Cilden-Guler, D., Kaymaz, Z., and Hajiyev, C. (2019). Assessment of Magnetic Storm Effects under Various Magnetometer Noise Levels for Satellite Attitude Estimation. In *9th International Conference on Recent Advances in Space Technologies (RAST)* pp. 769–773. https://doi.org/10.1109/RAST.2019.8767834

Inamori, T, Sako, N., and Nakasuka, S. (2010). Strategy of Magnetometer Calibration for Nano-Satellite Missions and In-Orbit Performance. *AIAA Guidance, Navigation, and Control Conference*. Toronto, Ontario Canada.

Inamori, Takaya, Hamaguchi, R., Ozawa, K., Saisutjarit, P., Sako, N., and Nakasuka, S. (2016). Online Magnetometer Calibration in Consideration of Geomagnetic Anomalies Using Kalman Filters in Nanosatellites and Microsatellites. *Journal of Aerospace Engineering*, *29* (6), 04016046. https://doi.org/10.1061/(ASCE)AS.1943-5525.0000612

Inamori, Takaya, and Nakasuka, S. (2012). Application of Magnetic Sensors to Nano and Micro-Satellite Attitude Control Systems. In *Magnetic Sensors - Principles and Applications*. https://doi.org/10.5772/34307

Matandirotya, E., Van Zyl, R. R., Gouws, D. J., and Saunderson, E. F. (2013). Evaluation of a Commercial-Off-the-Shelf Fluxgate Magnetometer for Cube Sat Space Magnetometry. *Journal of Small Satellites*, *2* (1), 133–146. Retrieved from http://adsabs.harvard.edu/abs/2013JSSat...2..133M

Psiaki, M. L., Martel, F., and Pal, P. K. (1990). Three-axis attitude determination via Kalman filtering of magnetometer data. *Journal of Guidance, Control and Dynamics*, *13* (3), 506–514. https://doi.org/10.2514/3.25364

Thébault, E., Finlay, C. C., Beggan, C. D., Alken, P., and Al., E. (2015). International Geomagnetic Reference Field: the 12th generation. *Earth, Planets and Space*, *67:69* . https://doi.org/10.1186/s40623-015-0228-9

Tsyganenko, N. A. (1989). A Magnetospheric Magnetic Field Model with a Warped Tail Current Sheet. *Planet. Space Science*, *37* (1), 5.

Tsyganenko, N. A. (1995). Modeling the Earth's Magnetospheric Magnetic Field Confined within a Realistic Magnetopause. *Journal of Geophysical Research*, *100* (A4), 5599–5612.

Tsyganenko, N. A. (2002). A model of the near magnetosphere with a dawn-dusk asymmetry 1. Mathematical structure. *Journal of Geophysical Research: Space Physics*, *107* (A8), SMP 12-1-SMP 12-15. https://doi.org/10.1029/2001JA000219

Tsyganenko, N. A. (2008). Modeling the Earth's Magnetosphere Using Spacecraft Magnetometer Data. Retrieved from http://geo.phys.spbu.ru/~tsyganenko/modeling.html

Wertz, J. R. (1988). *Spacecraft Attitude Determination and Control*. *Astrophysics and Space Science Library*. Kluwer Academic Publishers, Dordrecht, Holland.

Zhang, Z., Xiong, J., and Jin, J. (2015). On-orbit real-time magnetometer bias determination for micro-satellites without attitude information. *Chinese Journal of Aeronautics*, *28* (5), 1503–1509. https://doi.org/10.1016/J.CJA.2015.08.001